The Astronomical Journal, 128:2510–2517, 2004 November


# TILTING SATURN. II. NUMERICAL MODEL

Douglas P. Hamilton
Department of Astronomy, University of Maryland, College Park, MD 20742-2421; hamilton@astro.umd.edu

and

William R. Ward
Department of Space Studies, Southwest Research Institute, Suite 400, 1050 Walnut Street, Boulder, CO 80303; ward@boulder.swri.edu

*Received 2003 December 30; accepted 2004 July 15*

## ABSTRACT

We argue that the gas giants Jupiter and Saturn were both formed with their rotation axes nearly perpendicular to their orbital planes, and that the large current tilt of the ringed planet was acquired in a post-formation event. We identify the responsible mechanism as trapping into a secular spin-orbit resonance that couples the angular momentum of Saturn's rotation to that of Neptune's orbit. Strong support for this model comes from (1) a near-match between the precession frequencies of Saturn's pole and the orbital pole of Neptune, and (2) the current directions that these poles point in space. We show, with direct numerical integrations, that trapping into the spin-orbit resonance and the associated growth in Saturn's obliquity are not disrupted by other planetary perturbations.

*Key words:* planets and satellites: individual (Neptune, Saturn) — solar system: formation — solar system: general

*Online material:* color figures

## 1. INTRODUCTION

The formation of the solar system is thought to have begun with a cold interstellar gas cloud that collapsed under its own self-gravity. Angular momentum was preserved during the process, so that the young Sun was initially surrounded by the solar nebula, a spinning disk of gas and dust. From this disk, planets formed in a sequence of stages whose details are still not fully understood. One stage that both Jupiter and Saturn, large planets with nearly solar compositions, must have undergone, however, is the direct accretion of gas from rotating subnebulae. In the simplest models, the vast majority of the gaseous material making up Jupiter and Saturn flowed through these accretion disks, which should have been coplanar with the solar nebula. Conservation of angular momentum in this formation scenario predicts spin axes for these planets that are nearly perpendicular to their orbital planes, and indeed, Jupiter's tilt is only $3\overset{\circ}{.}1$. Saturn, however, has an obliquity of $26\overset{\circ}{.}7$, in apparent contradiction to this likely formation scenario.

The cleanest way out of this paradox is to invoke an additional process to tip Saturn after its accretion was essentially complete. Two main possibilities have been suggested previously: giant impacts (Lissauer & Safronov 1991; Parisi & Brunini 2002) and an external torque on the entire solar system (Tremaine 1991). The requirements for each of these hypotheses are rather strict, and at present there seems to be no clear way to test either one. Here and in a companion paper (Ward & Hamilton 2004, hereafter Paper I), we suggest an alternative evolutionary process that tilted Saturn subsequent to its formation: a secular spin-orbit resonance with the planet Neptune. Our preceding paper treated this scenario analytically using the Cassini state formalism originally developed by Colombo (1966) and explored by Peale (1969), Ward (1975), and others. The critical simplifying assumption underlying our analytical study is that Saturn's orbit can be treated as being of constant inclination, precessing at a uniform rate because of perturbations from Neptune. In reality, Saturn's inclination varies, its precession is nonuniform, and the instantaneous perturbations from Jupiter are larger than those from Neptune. In order to determine if our assumption is valid for the real solar system, we have developed a numerical model that includes the effects of all of the giant planets. And to facilitate a comparison between the output of our numerical model, our analytical results, and the real solar system, we have developed a useful analogy with orbital resonances.

## 2. CASSINI STATES

Torques imparted by the Sun on the oblate figure of Saturn cause slow, uniform precession of the planet's spin axis around its orbit normal. In the absence of planetary perturbations, all values of Saturn's obliquity would be stable solutions, each with its own precession rate. In reality, however, the gravitational perturbations of the other planets force Saturn's orbit to precess about the total angular momentum vector of the solar system. Orbital precession modulates the solar torque in time and rules out uniform spin-axis precession at most values of the obliquity. But if the planet's orbital precession is uniform, as would be the case with a single perturbing planet, there are several solutions that lead to uniform polar precession at constant obliquity. These are Cassini states, formal obliquity equilibria in which the precession rate of the planet's spin axis exactly matches that of its orbital plane (Colombo 1966; see also Fig. 1 of Paper I).

In the real solar system, however, Saturn's orbital precession rate is not uniform but is, rather, composed of multiple frequencies induced primarily by the other giant planets. Jupiter's perturbations dominate, and accordingly, it is not immediately obvious that the evolution of Saturn's spin axis due to Neptune can be treated with the Cassini state formalism, especially since Neptune's effects are an order of magnitude weaker than Jupiter's.

With orbital mean motion and secular resonances, however, it is often an excellent approximation to ignore all rapidly

varying terms in the perturbation potential while retaining only the slowly varying, near-resonant ones (see, e.g., Murray & Dermott 1999, p. 332). The rationale for this approximation is that the rapidly varying terms tend to average out over time, while the slowly varying terms can build up large amplitude changes to an orbit. We proceed in a similar manner here, neglecting all terms that affect Saturn's orbit but the one due to the $g_{18}$ fundamental frequency of the solar system, which is dominated by Neptune's nodal precession. This term has a period of $T_g = 1.87$ Myr (Applegate et al. 1986; Bretagnon 1974), a close match to the theoretical precession period of Saturn's pole at $T_\alpha \approx 1.8$ Myr (Tremaine 1991; French et al. 1993). While the uncertainty in $T_g$ is only a few tenths of a percent (Laskar 1988), $T_\alpha$ is known only to within several percent, with the greatest uncertainty coming from Saturn's moment of inertia (Paper I). French et al. (1993) combined *Voyager* measurements and the 1989 July occultation of the star 28 Sgr to actually measure Saturn's slow polar precession rate. Their results are consistent with the theoretical expectation, with estimated errors of approximately 35% dominated by uncertainties in the trajectories of the *Voyager* spacecraft. The poorly constrained value of $T_\alpha$ allows the possibility $T_g = T_\alpha$ required by the Cassini state.

How close is Saturn's pole to a Cassini state if all orbital perturbations but those due to Neptune's $g_{18}$ term are ignored? In addition to identical precession periods, in a Cassini state the vectors $\boldsymbol{s}$ (Saturn's north pole), $\boldsymbol{n}$ (Saturn's orbit normal), and $\boldsymbol{k}$ (the unit vector along the total angular momentum of the solar system about which both $\boldsymbol{s}$ and $\boldsymbol{n}$ precess) must all be coplanar (Colombo 1966). Saturn's pole direction $\boldsymbol{s}$ is given by R.A. $= 40\overset{\circ}{.}5954$ and decl. $= 83\overset{\circ}{.}538$ in the Earth equatorial coordinate system (epoch J2000.0), and in the same system, the normal to the invariable plane of the solar system $\boldsymbol{k}$ is given by R.A. $= 273\overset{\circ}{.}8657$ and decl. $= 66\overset{\circ}{.}9723$ (Yoder 1995). In addition, Neptune's perturbation on Saturn's orbital plane has an amplitude of $I = 0\overset{\circ}{.}0644$ and a phase of $\Omega = 23\overset{\circ}{.}52$ relative to the invariable plane, according to fits to 100 Myr numerical simulations of the outer solar system by Applegate et al. (1986). The Applegate values agree to better than a percent with the analytic theories of Bretagnon (1974), Laskar (1988), and Bretagnon & Francou (1992).

We now rotate $\boldsymbol{s}$ into invariable coordinates so that all three poles are defined in the same system. The resulting configuration of poles is close to Cassini state 2, depicted in Figure 1 of Paper I. In Cassini state 2, $\boldsymbol{n}$, $\boldsymbol{k}$, and $\boldsymbol{s}$ all lie in a single plane with $\boldsymbol{k}$ between $\boldsymbol{n}$ and $\boldsymbol{s}$. We project $\boldsymbol{k}$ and $\boldsymbol{s}$ into the plane perpendicular to $\boldsymbol{n}$ and determine the angle between the projections as follows:

$$\sin \Psi_{\rm Saturn} = \frac{(\boldsymbol{k}\times\boldsymbol{n})\times(\boldsymbol{s}\times\boldsymbol{n})}{|\boldsymbol{k}\times\boldsymbol{n}||\boldsymbol{s}\times\boldsymbol{n}|}. \quad (1)$$

With the pole directions given above, we find $\Psi_{\rm Saturn} = -31^\circ$. Thus, Saturn's pole, while not precisely in Cassini state 2, is close enough that it could be undergoing stable librations.

## 3. NUMERICAL MODEL

In this section, we describe the development of a self-consistent numerical model of the dynamics of Saturn's spin axis that includes two primary components: a detailed synthetic model for the varying orbits of the outer planets due to Bretagnon (see, e.g., Bretagnon & Francou 1992), and equations accurate to fourth order in the orbital elements for the evolution of the Saturnian spin axis from Ward (1979).

The outer-planet model of Bretagnon can be understood as large Fourier series fits to the time variations of each of the six orbital elements of each of the four giant planets. The actual variations of the orbital elements were obtained from a 1 Myr full numerical integration of the motions of the giant planets done in ecliptic coordinates. The allowed frequencies of the Fourier series were chosen to be all possible linear combinations of the 12 fundamental frequencies of the four giant planets. Four of these frequencies are simply the planetary mean motions, which dominate changes in the mean longitudes. The other eight are longer period secular frequencies that primarily affect orbital nodes and pericenters. The full outer-planet model includes 1300 frequencies that determine the motions of Saturn's pericenter and 127 that affect its node. Of these, 143 (pericenter) and 64 (node) are fully secular terms that do not involve planetary orbital frequencies. Inclusion of all terms in Bretagnon's full model ensures an accuracy of a few parts in $10^5$ for the time variations of the planetary semimajor axes, eccentricities, and inclinations over a million years.

To obtain the ecliptic orbital elements of Saturn at any given time, we simply determine the instantaneous phases of all of the relevant Fourier terms in Bretagnon's theory, compute the instantaneous contributions of these terms to each of Saturn's orbital elements, and sum over all of the contributions. These orbital elements are then used to determine the right-hand side of the vector equation of motion that governs the evolution of the unit spin vector as given by Ward (1979, eq. [6]). This equation is accurate to fourth order in the planetary eccentricity and inclination, which is sufficient since these quantities remain small throughout Saturn's orbital evolution. The dominant contribution to changes in Saturn's spin vector are first-order in the planet's inclination. This follows from the fact that Saturn's inclination determines the normal to its orbit, from which the obliquity is measured. By contrast, changes in Saturn's eccentricity affect the spin-axis evolution more weakly by altering the average Saturn–Sun distance, which in turn slightly affects the spin-axis precession rate.

The equation of motion for Saturn's spin vector depends on its instantaneous value, which we transform into ecliptic coordinates. We then integrate the equation using one of two fourth-order adaptive step-size integration methods: Bulirsch-Stoer or Runge-Kutta (Press et al. 1989). We have run these integration schemes against one another as a basic test of the validity of our code. The output from our integration scheme is the spin-axis pointing in ecliptic coordinates as a function of time. Finally, we convert the spin-axis pointing into a coordinate system with Saturn's instantaneous orbit as the reference plane.

The speed of the numerical integrations is strongly affected by the large number of terms needed to calculate the instantaneous orbital elements and especially by the frequencies of the strongest rapidly varying terms. To maintain a given accuracy, the integration step size is automatically chosen to resolve these terms. A significant speedup in integration time is realized by working with only secular terms with characteristic timescales of tens of thousands of years, as opposed to terms involving mean motions, which vary on the orbital timescales of decades. Our neglect of these rapidly varying terms is justified by the long timescales, $T_\alpha \approx 1.8$ Myr, that we are primarily interested in. Furthermore, we find that we still obtain inclinations accurate to a few parts in $10^3$ and eccentricities accurate to a few percent by summing over only the secular terms. In fact, even limiting the frequencies to the 10 dominant ones comprised by the secular theory of Brouwer & van Woerkom (1950) does not degrade the solution significantly.

Brouwer & van Woerkom's secular model is reprinted by Murray & Dermott (1999, p. 303). There are three periodic terms that affect planetary nodes: $g_{16}$, arising primarily from the mutual Jupiter-Saturn perturbation; $g_{17}$, due mainly to Uranus; and $g_{18}$, dominated by Neptune. An additional term with zero frequency accounts for the tilt of the ecliptic relative to the invariable plane of the solar system. The Brouwer & van Woerkom model also includes six frequencies that affect orbital pericenters: a fundamental mode dominated by each of the giant planets and two long-period terms whose amplitudes are enhanced by the near-5:2 resonance between Jupiter and Saturn.

In each of the simulations presented in § 5, we use just the 10 Brouwer & van Woerkom frequencies to compute Saturn's orbital elements, although we have also run each of them with all of the 207 secular frequencies, with no differences that are discernible on a plot. In most tests, final obliquities and resonant angles differ by less than 1 part in $10^4$.

## 4. RESONANCES

In this section we derive some basic analytic results that will provide a straightforward way of interpreting our numerical simulations.

### 4.1. *Equations of Motion*

The vector equation of motion that governs the evolution of the spin-axis direction in a reference frame that precesses uniformly about $\boldsymbol{k}$ is given by Colombo (1966, eq. [12]) and also in Paper I. We resolve this equation into spherical coordinates in a reference frame with $\boldsymbol{z}$ along $\boldsymbol{n}$ as in § 2. We define the resonance angle by

$$\Psi = \phi_\alpha - \phi_g, \tag{2}$$

where $\phi_\alpha$ and $\phi_g$ are angles measured positively from a reference direction to the projections of $\boldsymbol{s}$ and $\boldsymbol{k}$ into the $x$-$y$ plane, respectively. We define $\cos I = \boldsymbol{n} \cdot \boldsymbol{k}$ and $\cos\theta = \boldsymbol{s} \cdot \boldsymbol{n}$, where $I$ is the strength of Neptune's perturbation on Saturn's orbital plane and $\theta$ is Saturn's obliquity, the instantaneous tilt of Saturn's pole vector from its orbital pole. Making the approximation $\theta \gg I$, which is satisfied for Cassini states 2 and 4 (but not state 1), we find the following simple expressions for the time evolution of the resonant angle and obliquity:

$$\frac{d\Psi}{dt} = -\alpha\cos\theta - g\cos I, \tag{3}$$

$$\frac{d\theta}{dt} = g\sin I\sin\Psi \tag{4}$$

(compare with the more general expressions in Ward 1974). Here $t$ is time, $\alpha > 0$ is the precessional constant, which depends on Saturn's spin rate and oblate shape and the Sun's mass and distance (see eq. [1] of Paper I), and $g = g_{18} < 0$ is the nodal precession rate of Saturn's orbit induced by Neptune. To this level of approximation $\cos I \approx 1$, but we have retained the cos $I$ term to preserve the symmetric appearance of the two equations. In the limit $g = 0$, Neptune's perturbations vanish, Saturn's orbit plane becomes fixed in space, and we recover simple precession of the pole vector at a constant obliquity with period $T_\alpha = 2\pi/(\alpha\cos\theta)$. Note that since $\alpha > 0$, Saturn's pole precession rate is negative.[1]

A familiar application of equations (3) and (4) is to the tilt of Earth, with $T_g = 2\pi/|g|$ equal to the 18.6 yr regression of the lunar orbit due to solar perturbations and cos $I$ representing the strength of this perturbation to the motion of Earth's spin axis. The lunar torques affect Earth's obliquity through equation (4) and induce a rapid 18.6 yr nodding of Earth's spin axis (nutation) superposed on its more stately 25,800 yr precession.

For Neptune's perturbations on Saturn, the two terms on the right-hand side of equation (3) nearly cancel ($-g \approx \alpha\cos\theta$)—this can be thought of as a commensurability (or near-resonance) between the precession and nutation periods. In this case, equation (3) shows that $\Psi$ will vary slowly in time, which in turn allows large obliquities to build up via equation (4). This pair of equations is strongly reminiscent of the equations governing a first-order mean motion resonance between two planets (e.g., Hamilton 1994, eq. [29]), with the obliquity $\theta$ taking the place of either the orbital eccentricity or inclination. As with orbital mean motion resonances, here a single forcing frequency $g$ dominates the motion of Saturn's pole because of its near-match to the system's natural frequency ($-\alpha\cos\theta$).

Taking the time derivative of equation (3) and using equation (4) to eliminate $d\theta/dt$, we find

$$\frac{d^2\Psi}{dt^2} = (\alpha g\sin\theta\sin I)\sin\Psi - (\dot\alpha\cos\theta + \dot g\cos I), \tag{5}$$

which is qualitatively similar to a pendulum equation for $\Psi$. Here we have explicitly left in $\dot\alpha$ and $\dot g$, the slow tuning of the frequencies $\alpha$ and $g$ that took place during the early evolution of the solar system. Although $\alpha\cos\theta \approx -g$ today, this was not always the case. The precessional constant $\alpha$, which parameterizes the strength of the solar torque on Saturn's oblate figure and its regular satellites, decreased in the early solar system ($\dot\alpha < 0$) for several reasons: (1) the Kelvin-Helmholtz contraction of Saturn as it cooled, (2) the dissipation of the disk out of which Saturn's satellites condensed, and (3) the small outward migration of Saturn that accompanied the clearing of the planetesimal disk. Similarly, the magnitude of Neptune's frequency $|g|$ has also diminished in time, as many Earth masses of material in the outer solar system were expelled from the solar system and the planetary orbits diverged as a consequence (Hahn & Malhotra 1999). More mass in the early solar system, as well as smaller distances between planets, results in shorter orbital precession timescales than prevail today. These slow evolutionary processes, acting in combination, brought the two precession periods ($T_\alpha$ and $T_g$) together from initially disparate values.

Equation (5) supports orbits in which $\Psi$ circulates through a full $2\pi$ (these have initial conditions with large positive or negative $d\Psi/dt$). These regions are divided from librating orbits, in which $\Psi$ oscillates through a more limited range of values, by a separatrix orbit with an infinite orbital period that traverses an unstable equilibrium point. Crossing the separatrix—resonance passage—can occur when parameters of the pendulum equation are changed, either slowly or abruptly; this can lead to trapping of $\Psi$ into libration or a jump across the libration region with accompanying strong kicks to the

[1] There is an interesting parallel between the negative precession rates of planetary pole vectors ($d\Psi/dt = -\alpha\cos\theta$) and satellite orbit planes ($d\Omega/dt = -X\cos i$), where $\Omega$ is the ascending node, $X$ is a strength constant, and $i$ is the orbital inclination. This parallel arises because both the planet and the satellite orbit may be treated as oblate objects subject to external torques.

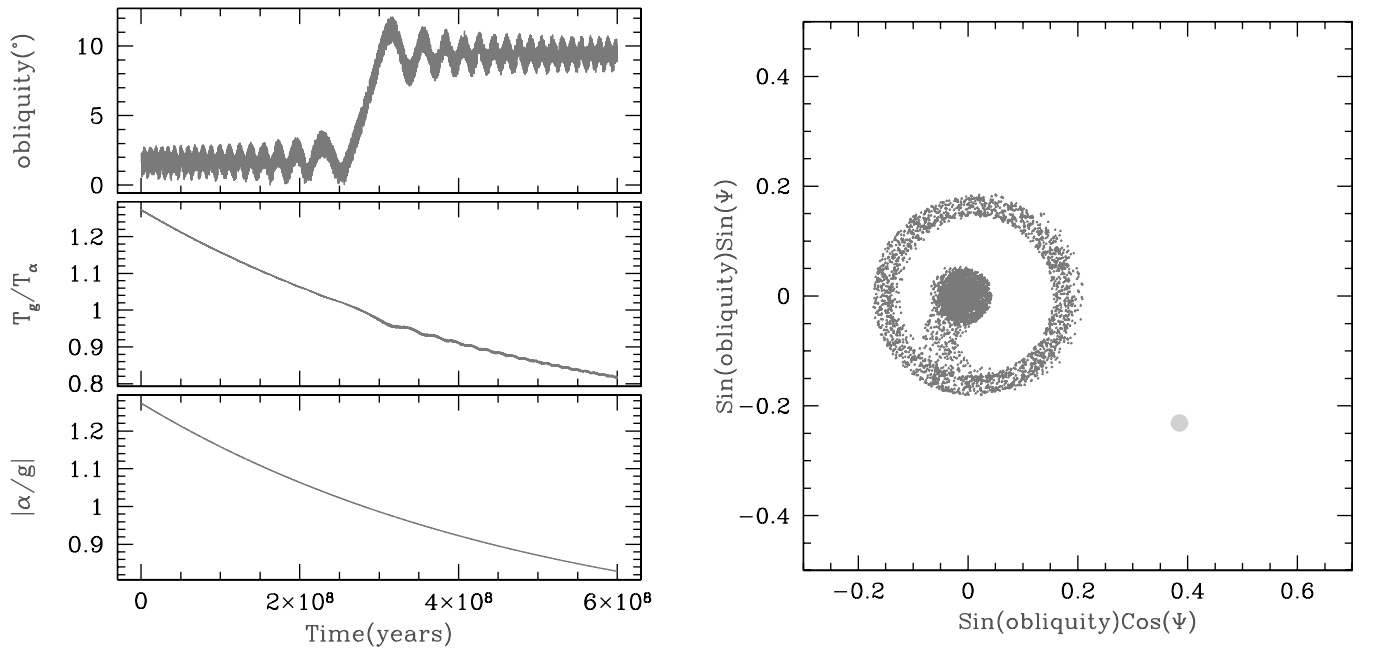


FIG. 1.—Resonant kick. *Left*: The obliquity $\theta$, the ratio of Neptune's orbital precession period $T_g$ to Saturn's spin precession period $T_\alpha$, and the absolute value of $\alpha/g$ vs. time. *Right*: Evolution of the resonant angle $\Psi$ (angle from the $x$-axis) and the obliquity $\theta$ (distance from the origin). Saturn's current pole position ($\Psi_{\rm Saturn} = -31\overset{\circ}{.}0$ and $\theta_{\rm Saturn} = 26\overset{\circ}{.}7$; see § 2) is indicated with a large dot. In these simulations, we impose the time history of $|\alpha/g|$ and study the response of the other variables. Here we have set $g$ constant, $\alpha = -0.64g(1 + e^{-t/\tau})$ with $\tau = 5\times10^8$ yr, and the initial condition $\theta_0 = 2\overset{\circ}{.}5$.

obliquity. Similar behavior is displayed by orbital mean motion resonances that also obey pendulum-like equations.

Equation (5) admits two equilibrium points, a stable one located at $\Psi_{\rm eq}$ and an unstable one at $\Psi_{\rm eq} + \pi$, where, assuming small $\dot\alpha$ and $\dot g$,

$$\Psi_{\rm eq} = \frac{\dot\alpha\,\cos\theta + \dot g\cos I}{\alpha g \sin\theta \sin I}. \tag{6}$$

When $g$ and $\alpha$ are constant, $\Psi_{\rm eq} = 0$, and the stable and unstable equilibrium points are identified with Cassini states 2 and 4, respectively. Treating $\theta$, $\dot\alpha$, and $\dot g$ as constants and assuming small-amplitude oscillations ($\sin\Psi \approx \Psi$), the solution to equation (5) is

$$\Psi = A\cos(w_{\rm lib}t + \theta) + \Psi_{\rm eq}, \tag{7}$$

where $A$ is the libration amplitude, $\theta$ is a phase, and $w_{\rm lib}$ is the libration frequency, given by

$$w_{\rm lib} = \sqrt{-\alpha g \sin\theta \sin I} \tag{8}$$

(recall that $g < 0$). For small-angle oscillations, the libration frequency is nearly constant and its value depends on properties of both the precessing planet and the perturbing term. In particular, just as for a simple pendulum, the libration frequency scales with the square root of the amplitude of the applied force, here $\sin I$. Furthermore, the libration frequency depends on $\sqrt{\theta}$ for small $\theta$ in just the same way that the libration amplitude for first-order mean motion resonances depends on $\sqrt{e}$. For current Saturn parameters, the period of these librations is $2\pi/w_{\rm lib} = 83$ Myr, which is much longer than the pole precession period.

## 5. NUMERICAL RESULTS

Processes active in the early solar system caused Saturn's pole precession rate to slow with time so that $\dot\alpha < 0$. If the frequency changed enough so that $\alpha \approx -g$ at some point, then a resonance passage should have occurred as discussed above. We simulate this scenario in Figure 1 by starting Saturn's pole precessing faster than Neptune's orbit ($|\alpha/g| > 1$) and allowing the pole precession rate to slow so that the ratio of precession periods approaches unity. As $|\alpha/g|$ approaches 1 the obliquity oscillations grow, and in a single libration period, the resonance imparts a $10^\circ$ kick to the obliquity. Although this sharp change in the obliquity affects the pole precession period somewhat, the period ratio $T_g/T_\alpha$ continues to decrease after the obliquity kick.

A tilt of $\theta = 10^\circ$ is significantly smaller than Saturn's current obliquity and also less than the maximum possible obliquity kick of $14\overset{\circ}{.}5$ from Paper I's equation (16). Note that the kick occurs when $\Psi \approx -110^\circ$ (Fig. 1, *right*), a value for which equation (4) predicts nearly the maximum effect on the obliquity. The kick is smaller than the maximum because $|\alpha/g|$ changes significantly over the libration period of the resonance, which violates the adiabatic condition and leads to smaller kick amplitudes as described by Paper I's equation (A4).

The apparent thickness of the obliquity versus time plot is due to rapid variations about an equilibrium value with an amplitude of around $1^\circ$. The perturbations of Jupiter on Saturn's orbital plane with $2\pi/g_{16} \approx 50{,}000$ yr and amplitude $0\overset{\circ}{.}9$ account for almost all of the observed oscillation. These rapid changes are not retained in our simple analytic model. They affect the numerical runs by smearing $\theta$ by about $2^\circ$ throughout its evolution (Fig. 1, *left*); this term also accounts for much of the thickness of the circular ring in the right panel of Figure 1. Despite their presence, Jovian perturbations do not strongly affect the kick to the obliquity imparted by the secular resonance with Neptune.

An additional feature of our analytic approximations is apparent in Figure 1—note that the period of the obliquity oscillation lengthens as the resonance location is approached, and then shortens afterward in agreement with equation (3). The

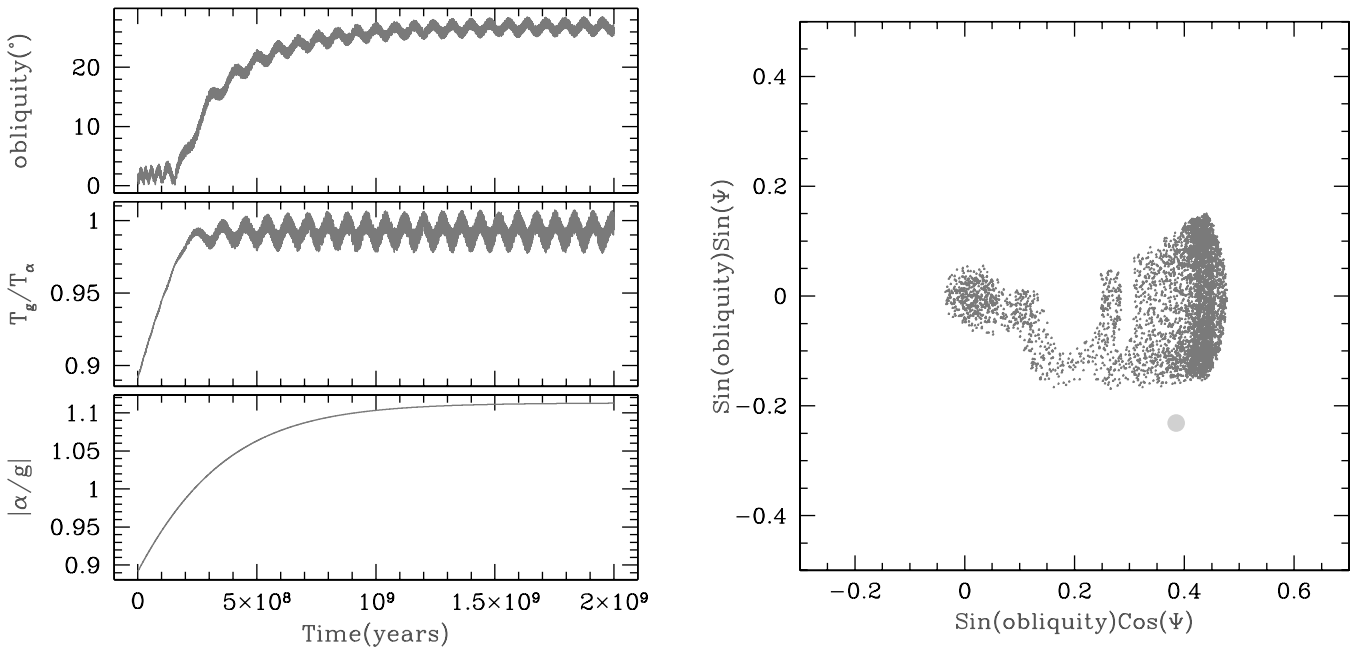


FIG. 2.—Trapping into resonance. Plotted quantities are as in Fig. 1. Here we have imposed $g = -\alpha(0.89 + 0.23e^{-t/\tau})$. Trapping into resonance occurs when the resonance angle librates through a limited range rather than circulating through a full $2\pi$. The ratio of precession periods pins to 1.

expression predicts that circulation of $\Psi$ in Figure 1 (*right*) is in the clockwise direction before the resonance obliquity is kicked (large $|\alpha/g|$) and counterclockwise afterward (small $|\alpha/g|$). This is just like a planar pendulum circulating in one direction that is slowed continuously until its motion reverses.

We have run a number of simulations, changing $|\alpha/g|$ at different rates and adjusting initial conditions so that the separatrix is met at different values of the resonance angle $\Psi$. In all cases, resonance kicks to the obliquity are limited to less than about 15°. Thus, an obliquity kick from Neptune's orbit is insufficient to explain the high obliquity of Saturn if the planet started close to an untilted state. Furthermore, as can be seen in Figure 1, after resonance passage the period ratio does not tend toward any particular value, nor is there a preferred value for the resonant angle. Even if the obliquity could reach 26.°7, the near-commensurability of the precession frequencies and the proximity of the observed resonant angle $\Psi_{\rm Saturn} = -31.°0$ to the stable equilibrium point $\Psi_{\rm eq} \approx 0$ would have to be attributed to chance. For all of these reasons, a simple kick to the obliquity is unable to explain the current state of Saturn's pole.

We turn now to investigate resonance trapping, which was possible during the clearing of the planetesimals from the outer solar system. Accordingly we take $\dot{g} > 0$ so that the ratio $|\alpha/g|$ increases with time. In Figure 2, we present a simulation in which we have tuned Neptune's precession frequency so that it ends with its current value, $|\alpha/g| \approx \cos 26.°7$. The obliquity starts small as in Figure 1, with the small-amplitude oscillations due to Jupiter's $g_{16}$ frequency. As the resonance with Neptune's orbital precession frequency is approached, equations (3) and (4) dominate the dynamics and resonance trapping occurs. The growth of the obliquity scales nearly as the square root of time for the portions of the evolution in which $|\alpha/g|$ is varying linearly. This growth after capture is also apparent in the right panel; the banana-shaped libration region expands outward and shifts slightly in the counterclockwise direction. The shift is due to the fact that $\Psi_{\rm eq} \to 0$ as $\theta$ increases and $\dot{g} \to 0$ (eq. [6]). Small oscillations in the obliquity occur at the libration period. Near the final obliquity, $\theta = 26.°7$, we measure 12.5 oscillations per $10^9$ years, for a libration period of 80 Myr. This is in good agreement with equation (8), which predicts an 83 Myr period.

The small offset of the stable equilibrium point $\Psi_{\rm eq}$ from zero when dissipation is present is the direct cause of the growth of the obliquity during resonance trapping. If $\Psi_{\rm eq} < 0$, as equation (6) and the right panel of Figure 1 show, then over one libration period the resonant angle spends more time at negative values than at positive ones, allowing the obliquity to increase irreversibly via equation (4). The characteristic growth timescale can be obtained by averaging over the libration period and inserting equation (6) into equation (4). If we assume low obliquity and slow linear changes of $\alpha$ and $g$ with time, we find that, in resonance, the obliquity varies with time in the following manner:

$$\theta = \sqrt{\theta_0^2 + 2(\dot{\alpha} + \dot{g})t/\alpha}, \tag{9}$$

where $\theta_0$ is the obliquity at $t = 0$. This expression is identical in form to Hamilton's (1994) equation (33), which was derived under similar approximations for orbital mean motion resonances. Equation (9) predicts the characteristic square-root-in-time growth of the obliquity for $\dot{\alpha} + \dot{g} > 0$. If the current 26.°7 obliquity of Saturn arose from resonance trapping, then the required frequency shift is $\Delta g = (1 - \cos 26.°7)g \approx \dot{g}t \approx 0.11g$, a change in the fundamental frequency of just over 10%.

Although this simulation nicely reproduces Saturn's current tilt, it is not consistent with the planet's current pole vector. The libration of the resonant angle displayed in the right panel of Figure 2 is too small to encompass the current pole vector of Saturn; a larger libration amplitude is needed. We have run many numerical experiments to see how the magnitude of the libration amplitude depends on various initial conditions. For a slow transition into resonance, an adiabatic invariant

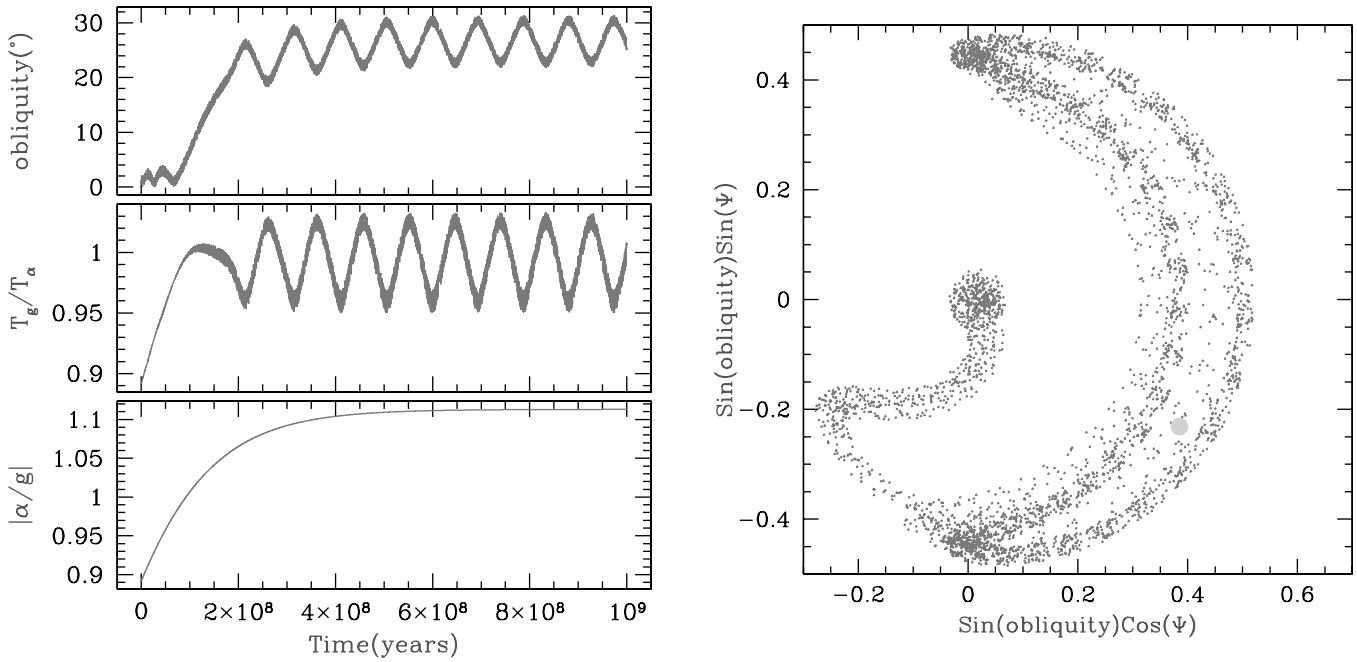


FIG. 3.—Rapid trapping into resonance. Plotted quantities are as in Fig. 1. The libration period is measured to be 83.3 Myr. Large libration amplitudes such as this are possible when the timescale for a characteristic change to the system is comparable to the libration period. Such rapid changes violate the adiabatic condition.

determines the final libration amplitude from the obliquity immediately prior to resonance capture (Paper I). Crudely, the area inside the circular region before trapping is preserved in the area swept out by the banana-shaped libration after trapping. Thus, in the adiabatic limit small initial obliquities necessitate small resonance libration amplitudes. There are two ways out of this dilemma. The first is simply to have the relevant frequency, here $g$, change rapidly enough that it changes its value significantly in one libration period, the characteristic timescale in resonance. A rapid change invalidates the adiabatic invariant.

Figure 3 is an example of resonance trapping, but this time with a much faster change in $|\alpha/g|$. In this case, most of the growth of the obliquity occurs over a single libration period. Despite starting with a low obliquity of only a few degrees as in Figure 1, the final libration amplitude is quite large. The libration amplitude is directly related to the obliquity oscillations, as can be shown by considering the integral of the motion obtained by solving equations (3) and (4) for $d\Psi/d\theta$ and integrating. The result is

$$K = g \sin I \cos \Psi - g\theta \cos I - \alpha \sin \theta, \qquad (10)$$

where we have assumed that $\alpha$ and $g$ are constants. This expression is valid instantaneously for small adiabatic changes to $g$ and $\alpha$. It can be used to relate the maximum excursions in $\Psi$ and $\theta$ over one libration period. For small libration amplitudes, we find

$$\Delta\Psi = \sqrt{\tan\theta / \sin I}\, \Delta\theta, \qquad (11)$$

which, for the current values of $\theta$ and $I$, yields $\Delta\Psi \approx 21\, \Delta\theta$. This predicts that the 4° obliquity oscillations in the left panel of Figure 2 should lead to 84° oscillations in $\Psi$ in the right panel—not a bad match, given the small libration amplitude approximation made in deriving equation (11). The fact that Saturn's pole does not lie on the final path of libration is not a concern—a slight change to the final value of $|\alpha/g|$ (within actual uncertainties) moves the banana-shaped libration region either inward or outward so that it crosses the current pole position of Saturn. Thus this simulation is one possible past history of Saturn's pole—a fast passage through the resonance. A fast resonance passage can simultaneously account for the current tilt of Saturn and the $\Psi_{\rm Saturn} = -31\overset{\circ}{.}0$ offset of Saturn's pole vector from Cassini state 2.

Our numerical experiments show that it requires a fast resonance encounter, as well as a fortuitous phase $\Psi$ at the time of the encounter, to induce a large libration amplitude. The example in Figure 3 is near the limit of the fastest possible resonance capture. That such a limit must occur can be seen from equation (5) if the second term on the right dominates the first term for all $\Psi$. In this case, the equilibrium points given by equation (6) no longer exist. For changes to Neptune's orbital precession rate, trapping is no longer possible when $\dot{g} \approx w_{\rm lib}^2$. We find that Saturn's pole can be trapped with a libration amplitude larger than ≈30° for all rates from about a factor of 2 slower than in Figure 3 to just slightly faster.

An alternative path to large libration amplitudes involves a slower scanning rate of the frequencies and a larger initial obliquity. One way that Saturn might have had a larger obliquity before becoming trapped in the $g_{18}$ resonance is if it were kicked by other resonances or by the $g_{18}$ earlier in its history. In Figure 4, we impose a model that includes both Saturn's contraction on a rapid timescale and clearing of the planetesimal swarm on a slower timescale. The frequencies are brought together twice, first in the direction that leads to an obliquity kick as in Figure 1 and then in the direction that leads to resonance capture as in Figure 2. The planet acquires a 9° obliquity, which it maintains until meeting the resonance for the second time. The adiabatic invariant ensures that this initial

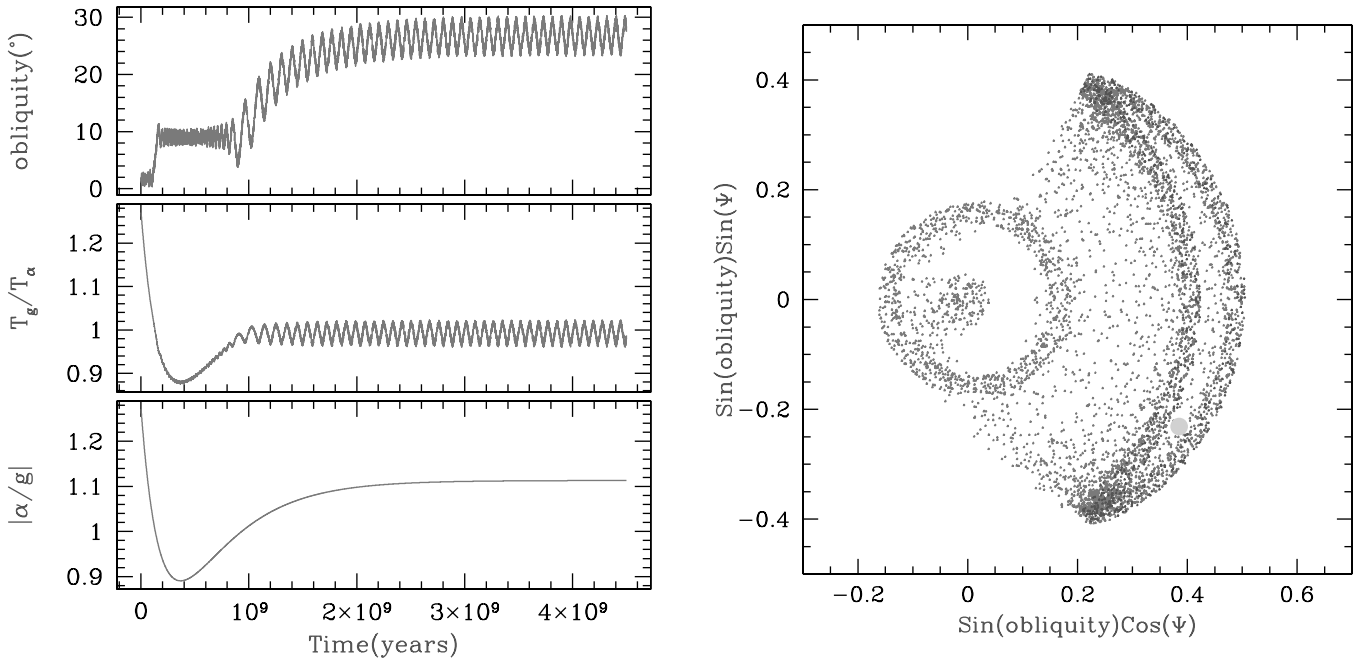


FIG. 4.—Kick followed by trapping into resonance. Plotted quantities are as in Fig. 1. Another way to achieve large libration amplitudes is to start with a large obliquity. Here we impose a model that first decreases $|\alpha/g|$ and brings it across the resonance in the direction that yields obliquity kicks. The model then causes $|\alpha/g|$ to increase so that the resonance is encounted again, this time from the opposite direction with a larger obliquity. Trapping with large libration amplitude ensues.

obliquity translates into a large libration amplitude (note that the areas inside the circle and inside the banana shape are similar).

Several additional features of Figure 4 warrant discussion. First note that the libration period near $t = 10^9$ yr, when $\theta \approx 12^\circ$ is clearly longer than the libration period at $\theta \approx 27^\circ$. More careful measurements of the libration period show that it shortens by a factor of about 1.5, in agreement with the $\theta$-dependence of the libration amplitude predicted by equation (8). The distribution of points plotted between the circle and banana shape is offset slightly in the clockwise direction as required by equation (6) during obliquity growth. Finally, the observed $\Delta\theta \approx 3.^\circ5$ and $\Delta\Psi \approx 60^\circ$ are reasonably consistent with the predictions of equation (11).

## 6. CONSTRAINTS ON THE EARLY EVOLUTION OF THE SOLAR SYSTEM

We have investigated the conditions under which trapping into the $g_{18}$ secular spin-orbit resonance is possible and shown that both (1) the observed near-match between the precession periods of Saturn's pole and Neptune's orbit and (2) the current pointing of Saturn's pole vector can be simultaneously explained by this mechanism. We believe that these successes make resonance capture the most likely explanation of Saturn's large obliquity. Trapping can be achieved by either (*a*) fast resonance passage or (*b*) a precapture obliquity of at least $4^\circ$ (Paper I).

Can the resonance-capture model place constraints on the processes active in the early solar system? Since Saturn first encountered the secular spin-orbit resonance with Neptune, the frequency ratio $\alpha/g$ has changed by about 10%, with the exact amount dependent on the initial obliquity as described by equation (9). This sets a lower limit on the amount of material that was swept from the outer solar system; Paper I estimates that removing about 10 Earth masses of material from the Kuiper belt would change $g$ by about 10%. Less material is required if the material is located between the planets, and if the changes to the planetary orbits due to the ejection of this mass are also considered.

The origin of Saturn's tilt also sets a lower limit on the amount of time required to remove the planetesimals, as a too-rapid change to the $g_{18}$ precession frequency precludes resonance trapping. The material must be removed over a time period exceeding about 150 million years, as seen in Figure 3. When did Saturn gain its large obliquity? First, solar system evolution must have slowed to the point where subsequent changes to the $g_{18}$ frequency were of order 10%. Processes that affect the solar system so drastically probably only occurred in the first $10^9$ or so years of its history. So Saturn was probably tilted to near its current obliquity sometime between 200 Myr and 1 Gyr after the formation of the solar system.

Because of the long libration period of the $g_{18}$ secular resonance, Saturn has undergone at most about 50 full librations over the age of the solar system. Accordingly, it is unlikely that dissipative processes internal to Saturn have had enough time to significantly damp the libration amplitude. Furthermore, because there are no strong forcing frequencies with extremely long periods (10–100 Myr), the $g_{18}$ term does not split into a multiplet of nearby resonances. Hence, resonance overlap and the associated chaotic evolution of the libration amplitude, which play an important role for the Kirkwood gaps in the asteroid belt (Wisdom 1987), are unlikely to be important for Saturn's pole. Thus, the pole's libration amplitude probably has not changed much over the past several gigayears. It might be determined by a more sensitive measurement of Saturn's pole precession rate or an improved model of the precession rate, whose largest uncertainty is in Saturn's moment of inertia. An accurately determined current libration amplitude would put potentially interesting additional constraints on the capture process and on the early history of the solar system.

We dedicate this work to the memory of Pierre Bretagnon, who tragically passed away on 2002 November 17. We wish to thank the anonymous reviewer for perceptive questions and comments, and Leslie Sage for a critical reading. Initial funding was provided by a Southwest Research Institute Quick-Look Grant awarded during D. P. H.'s sabbatical leave at SwRI in Boulder, Colorado. Additional support from an NSF Career Award (D. P. H.), NASA's Origins Program (D. P. H.), and NASA's Planetary Geology and Geophysics Program (W. R. W.) is gratefully acknowledged.

REFERENCES

Applegate, J. H., Douglas, M. R., Gürsel, Y., Sussman, G. J., & Wisdom, J. 1986, AJ, 92, 176
Bretagnon, P. 1974, A&A, 30, 141
Bretagnon, P., & Francou, G. 1992, in IAU Symp. 153, Chaos, Resonance and Collective Dynamical Phenomena in the Solar System, ed. S. Ferraz-Mello (Dordrecht: Kluwer), 37
Brouwer, D., & van Woerkom, A. J. J. 1950, The Secular Variations of the Orbital Elements of the Principal Planets (Astron. Pap. Am. Ephemeris Naut. Alm., 13, 81) (Washington: GPO)
Colombo, G. 1966, AJ, 71, 891
French, R. G., et al. 1993, Icarus, 103, 163
Hahn, J. M., & Malhotra, R. 1999, AJ, 117, 3041
Hamilton, D. P. 1994, Icarus, 109, 221
Laskar, J. 1988, A&A, 198, 341
Lissauer, J. J., & Safronov, V. S. 1991, Icarus, 93, 288
Murray, C. D., & Dermott, S. F. 1999, Solar System Dynamics (Cambridge: Cambridge Univ. Press)
Parisi, M. G., & Brunini, A. 2002, BAAS, 34, 892
Peale, S. J. 1969, AJ, 74, 483
Press, W. H., Flannery, B. P., Teukolsky, S. A., & Vetterling, W. T. 1989, Numerical Recipes in C (Cambridge: Cambridge Univ. Press)
Tremaine, S. 1991, Icarus, 89, 85
Ward, W. R. 1974, J. Geophys. Res., 79, 3375
———. 1975, AJ, 80, 64
———. 1979, J. Geophys. Res., 84, 237
Ward, W. R., & Hamilton, D. P. 2004, AJ, 128, 2501 (Paper I)
Wisdom, J. 1987, Icarus, 72, 241
Yoder, C. F. 1995, in Global Earth Physics, ed. T. J. Ahrens (Washington: Am. Geophys. Union), 1